Biosensors and Bioelectronics 53 (2014) 472–478

Contents lists available at ScienceDirect

Biosensors and Bioelectronics

journal homepage: www.elsevier.com/locate/bios

Amperometric cholesterol biosensor based on the direct electrochemistry of cholesterol oxidase and catalase on a graphene/ionic liquid-modified glassy carbon electrode

Mohammad Bagher Gholivand *, Mehdi Khodadadian

Department of Analytical Chemistry, Faculty of Chemistry, Razi University, Kermanshah, Iran

ARTICLE INFO

Article history:
Received 6 August 2013
Received in revised form
29 September 2013
Accepted 30 September 2013
Available online 21 October 2013

Keywords:
Graphene
Cholesterol oxidase
Catalase
Cholesterol
Electrocatalysis

ABSTRACT

Cholesterol oxidase (ChOx) and catalase (CAT) were co-immobilized on a graphene/ionic liquid-modified glassy carbon electrode (GR–IL/GCE) to develop a highly sensitive amperometric cholesterol biosensor. The H_2O_2 generated during the enzymatic reaction of ChOx with cholesterol could be reduced electrocatalytically by immobilized CAT to obtain a sensitive amperometric response to cholesterol. The direct electron transfer between enzymes and electrode surface was investigated by cyclic voltammetry. Both enzymes showed well-defined redox peaks with quasi-reversible behaviors. An excellent sensitivity of 4.163 mA mM^{-1} cm^{-2}, a response time less than 6 s, and a linear range of 0.25–215 μM ($R^2 > 0.99$) have been observed for cholesterol determination using the proposed biosensor. The apparent Michaelis–Menten constant (K_M^{app}) was calculated to be 2.32 mM. The bienzymatic cholesterol biosensor showed good reproducibility (RSDs < 5%) with minimal interference from the coexisting electroactive compounds such as ascorbic acid and uric acid. The CAT/ChOx/GR–IL/GCE showed excellent analytical performance for the determination of free cholesterol in human serum samples.

1. Introduction

Cholesterol is an essential lipid which found in the cell membranes of all animal and human cells and is the precursor for other biological materials such as steroid hormones. Normally, the concentration of free cholesterol in human serum is in the range 1.0–2.2 mM (Zhao et al., 2008). However, high cholesterol accumulation in blood due to excessive ingestion results in fatal diseases, such as arteriosclerosis, cerebral thrombosis, myocardial infarction, coronary diseases and lipid metabolism dysfunction, etc. (Ahmadalinezhad and Chen, 2011; Sugano and Beynen, 1990). The measurement of blood cholesterol concentration is a routine practice in medical screening or diagnosis. Various methods have been reported for the analysis of cholesterol in biological fluids including colorimetric, spectrophotometric, HPLC, and electrochemical methods (Krug et al., 1994; Nakaminami et al., 1997; Yao et al., 1995; Wong et al., 1994; Hojo et al., 2011). Among these, some methods often present certain disadvantages, such as lack of specificity and selectivity because of the interfering reactions and use of unstable and corrosive reagents (Brahim et al., 2001). However, because of their excellent specificity, enzymatic procedures have been practically preferred over chemical methods for the determination of cholesterol in biological samples (Gopalana et al., 2009).

Electrochemical biosensors have emerged recently as alternative tools for rapid and real-time analysis of clinically relevant analytes (Xu and Wang, 2012). These biosensors are rapid, easy to handle and are of low cost. Most of these devices are based upon the amperometric detection of hydrogen peroxide as the product of the enzymatic reactions. For example most of the cholesterol biosensors are based on the use of cholesterol oxidase (ChOx), a flavin adenosine dinucleotide (FAD)-containing enzyme, which catalyzes the oxidation of cholesterol to H_2O_2 and cholest-4-en-3-one in the presence of molecular oxygen (Ahn and Sampson, 2004). The electrochemical quantification of H_2O_2 would be convenient if the transducer can facilitate the redox process at a favorable potential without any interference from other coexisting analytes. However, previous studies show that at common solid electrodes the kinetic of electron transfer of H_2O_2 is sluggish and amperometric detection requires high applied potentials (Iannlello and Yacynych, 1981) that may induce simultaneous oxidation/reduction of other electroactive species in samples which may lead to false positive signals (Zhao et al., 2008). Hence, acceleration of redox process of H_2O_2 is necessary to develop any electrochemical biosensor which is based on the monitoring of enzymatically generated H_2O_2. Recently, many researchers have used nanostructured materials such as metal nanoparticles and carbon nanotubes

* Corresponding author. Tel.: +98 831 427 4557; fax: +98 831 427 4559.
E-mail address: mbgholivand@yahoo.com (M.B. Gholivand).

0956-5663/$ - see front matter © 2013 Elsevier B.V. All rights reserved.
http://dx.doi.org/10.1016/j.bios.2013.09.074

(CNTs) with catalytic effects to improve biosensor sensibility and to decrease the overpotential applied to the amperometric detection of H_2O_2 (Hall et al., 2000). However, many electrochemical techniques are based on the reduction of H_2O_2 by the catalysis of immobilized enzymes (peroxidases) to construct unmediated biosensors, which are based on the direct electron transfer between an electrode and immobilized enzyme (Ferapontova et al., 2001; Liu and Ju, 2002). It has been reported that proteins containing heme groups, such as hemoglobin, myoglobin and catalase (CAT) possess peroxidase like catalytic activity, which can reduce H_2O_2 due to the electroactive heme center (Gu et al., 2001; Liu et al., 2004) and have also been used for the preparation of H_2O_2 biosensors (Chen and Lu, 2006).

Graphene is a two-dimensional (2-D) sheet of carbon atoms in a hexagonal configuration with atoms bonded by sp^2 bonds (Novoselov et al., 2004). Graphene shows many advantages for electrochemical applications when compared to graphite or to carbon nanotubes. Graphene exhibits a surface area of 2630 $m^2 g^{-1}$, which is much greater than that of graphite ($\sim$10 $m^2 g^{-1}$) and even that of carbon nanotubes (1315 $m^2 g^{-1}$) (Pumera et al., 2009). The electrical conductivity of graphene is excellent. Electrodes made from graphene have significantly more uniform distribution of electrochemically active sites than do those made from graphite (Tan et al., 2010; Zhou et al., 2009). Therefore, graphene has exhibited potential applications in synthesizing nanocomposites and fabricating various electrical devices. Recently, its applications in biological and electrocatalytic aspects have boomed (Kang et al., 2009; Li et al., 2009).

Ionic liquids (ILs) are molten salts with the melting point close to or below room temperature. The good solvating properties, high conductivity, non-volatility, low toxicity, large electrochemical window and good electrochemical stability, make ILs suitable for many applications such as electrodeposition, electrosynthesis, electrocatalysis, electrochemical capacitors and lithium-ion batteries (Hapiot and Lagrost, 2008). Also ILs has been used as the modifier of the electrode or the binder to fabricate IL-carbon composites, typically for instance carbon ionic liquid electrode (CILE) (Safavi et al., 2009), IL-functionalized carbon nanotubes (Xiao et al., 2009), GR–IL hybrids (Yang et al., 2009), etc. Among these, the GR–IL based electrochemical sensors and biosensors have been recently reported for direct electron transfer and detection of different types of targets (Shan et al., 2010, 2009). These results suggest that GR–IL can remarkably increase the sensitivity and facilitate electron transfer of various redox biomolecules. Moreover, the combination of graphene sheets and IL via physical or chemical interactions can provide a more favorable micro-environment for the immobilization of enzymes/proteins, and IL can enhance their catalytic activity. The unique properties of both graphene and ionic liquid make this nanocomposite a promising platform for the construction of biosensors (Tunckol et al., 2012).

In this article, we attempt to propose a novel design for the bienzymatic cholesterol biosensor based on the co-immobilization of ChOx and CAT at the surface of a GR–IL modified GCE. The stable adsorption and direct electrochemistry of the two enzymes were observed at GR–IL/GCE. Through cooperation of the two enzymes, as well as the synergic effect of GR and IL, improved sensitivity and selectivity for cholesterol detection were achieved.

2. Experimental

2.1. Reagents and chemicals

ChOx (EC 1.1.3.6), CAT (EC 1.11.1.6), cholesterol and the ionic liquid 1-Butyl-3-methylimidazolium hexafluorophosphate ([bmim][PF_6]) were obtained from Sigma-Aldrich (Madrid, Spain). All other chemicals used were of analytical grade and used without further purification. Graphene oxide (GO) was prepared from graphite (Flakes) by the improved Hummers' method (Marcano et al., 2010). The GR–IL hybrid was prepared according to the literature (Yang et al., 2011a; Choi and Park, 2012). A mixture of GO/IL (95/5 w/w%) in 10 mL of deionized water was prepared. After sonication of the mixture for 60 min, the homogeneous solution was treated with 38 wt% hydrazine solution for reduction at 90 °C for 2 h. The resulting mixture was washed with deionized water several times and centrifuged to obtain GR–IL hybrid.

2.2. Instrumentation

Voltammetric measurements were carried out with an AUTOLAB (Eco Chemie B. V.) PGSTAT30 potentiostat/galvanostat. The electrochemical cell was assembled with a saturated Ag/AgCl reference electrode, a Pt wire auxiliary electrode, and the prepared working electrodes. The surface morphology of modified electrodes was characterized with a scanning electron microscope (SEM) (KYKY-EM3200).

2.3. Preparation of working electrodes

Glassy carbon electrodes were polished to a mirror-like surface with 1.0 and 0.3 μm alumina slurry, and then sonicated in water and ethanol, respectively. The ChOx/CAT/GR–IL/GCE was prepared as follows: briefly, a 10 μL of 1.0 mg/mL GR–IL suspension was spread on the surface of the electrode and dried at room temperature to form GR–IL modified GCE (GR–IL/GCE). After that, the GR–IL/GCE was separately incubated in 6 mg/mL CAT and 8 mg/mL ChOx in 0.01 M PBS (pH 7.4) each for 6 h at 4 °C to obtain ChOx/CAT/GR–IL/GCE. The mono-enzyme electrodes, i.e. CAT/GCE, ChOx/GCE, ChOx/GR–IL/GCE and CAT/GR–IL/GCE, were prepared in a similar way except that each electrode was only incubated in its corresponding enzyme solution. Finally, the electrodes were thoroughly rinsed with 0.01 M PBS (pH 7.4) to remove weakly adsorbed enzyme molecules.

2.4. Preparation of real samples

Free cholesterol in human serum samples was determined with the proposed cholesterol biosensor. A 0.5 mL serum sample was diluted to 10 mL with 0.01 M PBS (pH 7.4) containing 0.2% (v/v) Triton X-100 and 0.5% (v/v) isopropanol to make the cholesterol oncentrations fall in the linear range of the biosensor. The concentration of cholesterol was determined using standard addition method.

3. Results and discussion

3.1. Characterization of the modified electrode

Scanning electron microscopy (SEM) was employed to study the surface morphology of the modified electrode. Fig. 1A clearly shows that the GR–IL film has a typical crumpled and wrinkled structure of graphene sheet which provides a large rough surface for further immobilization of enzymes. When the electrode was incubated in the enzyme solution, the enzyme molecules adsorbed on the surface of GR–IL tended to aggregate as nanoparticles (white spots) throughout the surface which indicates the successful immobilization of enzymes on the GR–IL/GCE (Fig. 1B). Such behavior has been previously observed when glucose oxidase (GOD) and horseradish peroxidase (HRP) were immobilized on GR sheets (Yang et al., 2011a; Choi and Park, 2012). Non-covalent interactions such as π–π, π-cationic, ionic–ionic and/or hydrophobic–hydrophobic interactions

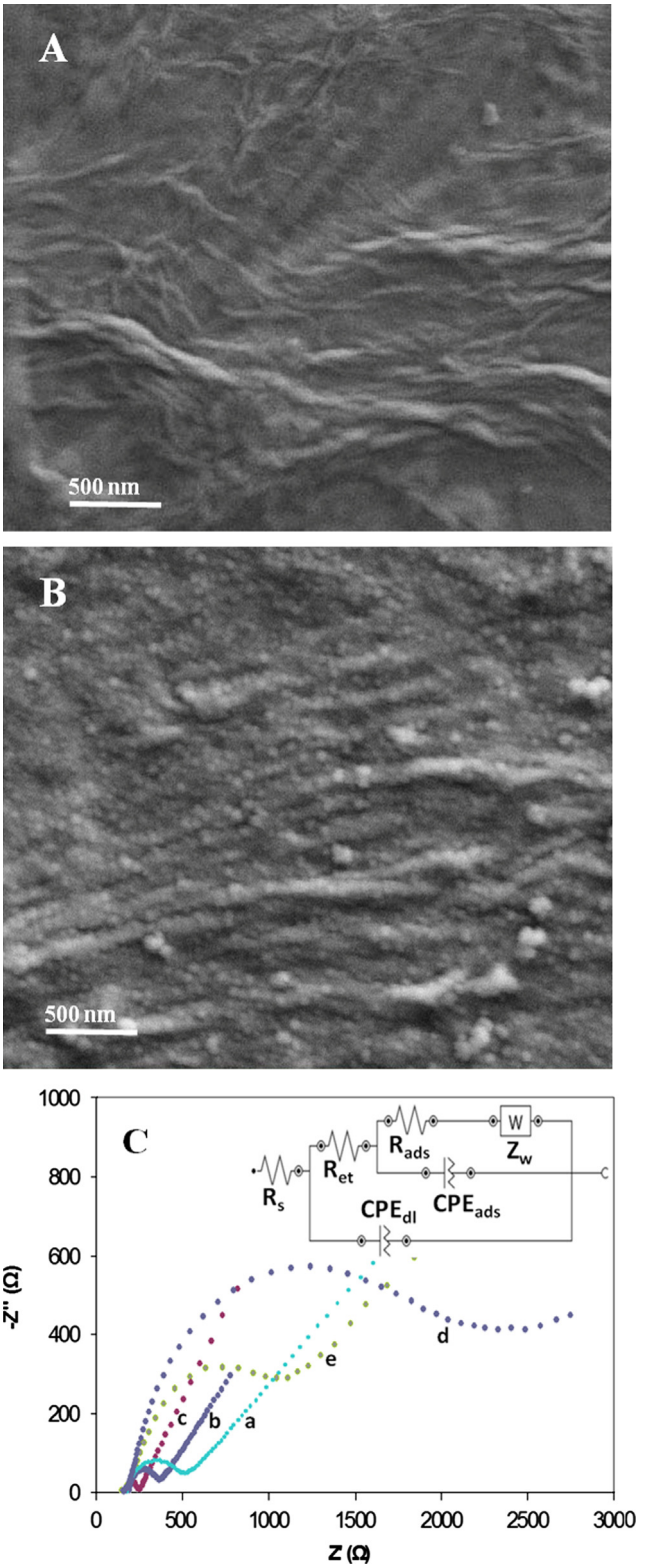

Fig. 1. (A) SEM images of GR–IL/GCE and (B) ChOx/CAT/GR–IL/GCE and (C) Nyquist plots obtained with different modified electrodes: (a) bare GCE, (b) GR/GCE, (c) GR–IL/GCE, (d) ChOx/CAT/GR/GCE, and (e) ChOx/CAT/GR–IL/GCE. The supporting electrolyte was a 0.01 M PBS (pH 7.4) solution containing 5.0 mM $[Fe(CN)_6]^{3-/4-}$ and 0.01 M KCl.

may contribute to the adsorption of enzymes on GR–IL surface (Tunckol et al., 2012).

The electronic transfer properties of the electrode after different surface modifications were characterized by electrochemical impedance spectroscopy (EIS). EIS is an effective technique for probing the features of surface modified electrodes. The impedance spectra include a semicircle portion and a linear portion. The semicircle diameter of well conducting substrates equals to the electron transfer resistance (R_{et}). In addition, the linear portion shows a controlled diffusion process. By using $[Fe(CN)_6]^{3-/4-}$ redox couples as the electrochemical probe, the Nyquist plots of different modified electrodes were obtained and the results are shown in Fig. 1C. The equivalent circuit compatible with the Nyquist plot is depicted in the inset of Fig. 1C. In this electrical equivalent circuit, R_s, CPE_{dl} and R_{ct} represent solution resistance, a constant phase element corresponding to the double layer capacitance and the charge transfer resistance. CPE_{ads} and R_{ads} are the electrical elements related to the adsorption of reaction intermediates. The value of R_{et} varies when different substances are present on the electrode surface. At the GCE, R_{et} can be estimated to be 420 Ω (curve a), indicating a relatively large electron transfer resistance. With the modification of graphene onto GCE, the diameter of the semicircle decreased (173 Ω) (curve b). It shows the consistency with the fact that graphene possesses high electrical conductivity which reduces the R_{et}. After assembling the GR–IL hybrid on the surface of GC electrode, the R_{et} was further decreased (49 Ω) (curve c), which may be due to the higher electrical conductivity of the GR–IL hybrid. In the case of ChOx/CAT/GR/GCE, the diameter of the semicircle portion was largely increased (1920 Ω) (curve d), indicating that the adsorption of CAT and ChOx on the GR layer leads to a great increase in electron transfer resistance. This may be due to the large molecular size of enzymes which hinders the access of the probe to the electrode surface. Finally, when the GR–IL hybrid was used instead of GR (ChOx/CAT/GR–IL/GC), the R_{et} decreased to 1010 Ω (curve e), implying that IL has a significant role in the electron transfer kinetic (Zhu et al., 2009). Therefore, the ChOx/CAT/GR–IL/GC electrode was used as a biosensor for detection of cholesterol.

3.2. Electrochemical behaviors of CAT and ChOx on GR/GC and GR–IL/GC electrodes

Fig. 2A shows the cyclic voltammograms (CVs) of 0.01 M PBS (pH 7.4) at the CAT/GC (a), CAT/GR/GC (b) and CAT/GR–IL/GC (c) electrodes. As seen, no apparent peaks were observed when CAT/GCE was immersed in 0.01 M PBS (pH 7.4) which confirms the previous report (Salimi et al., 2005). However, a pair of redox peaks with formal potential $[(E_{pa}+E_{pc})/2]$ about −0.480 V versus Ag/AgCl, which is the characteristic of catalase heme Fe(III)/Fe(II) redox couple (Melik-Adamyan et al., 1986; Salimi et al., 2005), was observed when CAT/GR/GC electrode was used. A similar result with an increase in height of both anodic and cathodic peak currents was observed when CAT/GR–IL/GC electrode was used. This is an indication for the fact that, the presence of GR–IL has a significant effect on the electron transfer reaction of enzyme via providing a suitable environment for the enzyme to transfer electrons to the surface of the electrode (Tunckol et al., 2012).

The effect of scan rate on the response of the CAT/GR–IL/GC electrode was investigated and the results are presented in Fig. S1 (Supporting information). The peak currents (I_{pa} and or I_{pc}) versus scan rate plots were linear and are depicted in Fig. S1(B) which reveals that the electrode reaction is a surface-confined redox process. Furthermore, by increasing the scan rate (10 to 250 mV/s) ΔE_p was increased from 20 to 75 mV with nearly constant peak current ratio suggesting that the electrochemical reaction of catalase on GR–IL/GCE corresponds to a quasi-reversible process (Bard and Faulkner, 2001). According to Laviron's model (Laviron, 1979) the peak potential separations at higher scan rates could be used to estimate the transfer coefficient (α) and the heterogeneous

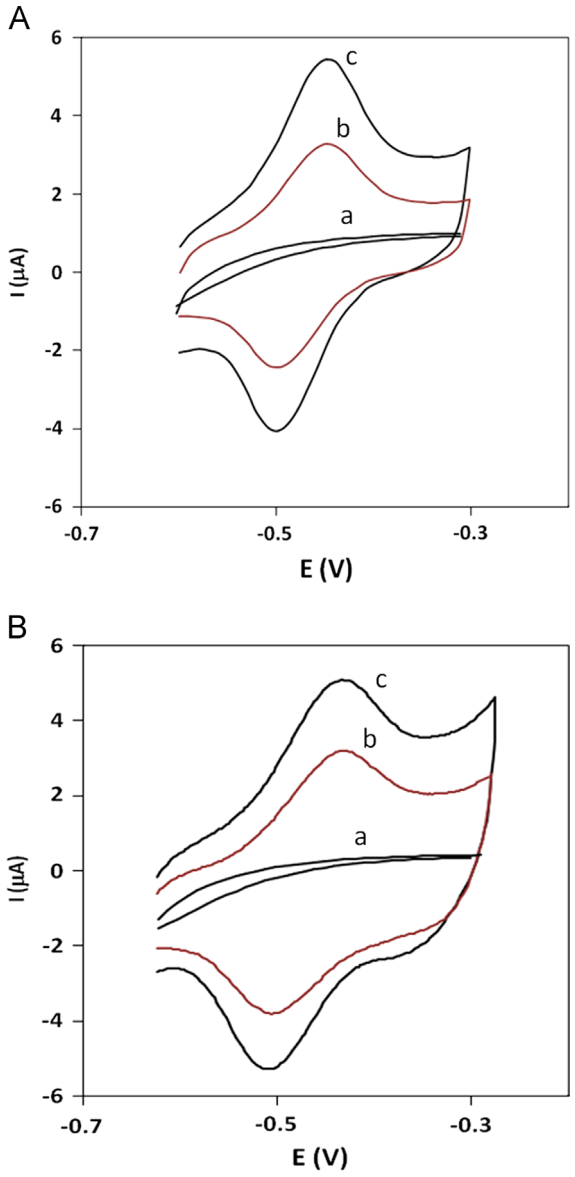

Fig. 2. (A) Cyclic voltammograms of (a) CAT/GCE, (b) CAT/GR/GCE and (c) CAT/GR–IL/GCE. (B) Cyclic voltammograms of (a) ChOx/GCE, (b) ChOx/GR/GCE and (c) ChOx/GR–IL/GCE. All voltammograms recorded at a scan rate of 100 mV/s in 0.01 M PBS (pH 7.4).

electron transfer rate constant (k_s):

$$E_{pc} = E^{0'} - 2.3RT\frac{\log\ \nu}{\alpha nF}$$

$$E_{pa} = E^{0'} + 2.3RT\frac{\log\ \nu}{(1-\alpha)nF}$$

$$\log\ k_s = \alpha\log(1-\alpha) + (1-\alpha)\log\ \alpha - \log\left(\frac{RT}{nF}\right) - \frac{\alpha(1-\alpha)nF\Delta E_p}{2.3RT}$$

where, α is the electron transfer coefficient, n is the electron transfer number, k_s is the apparent electron transfer rate constant, R is the gas constant, T is the absolute temperature, and ΔE_p is the peak-to peak separation. So, the values for α and k_s were evaluated as 0.61 and 2.60 s^{-1}, respectively. This rate constant is comparable to or higher than the apparent heterogeneous electron transfer rate constant of CAT at other modified electrodes (Zhang et al., 2001; Wu et al., 2006; Zhou et al., 2008; Chen et al., 2001; Li et al., 2004).

Also the electrochemical behaviors of ChOx/GCE, ChOx/GR/GCE and ChOx/GR/IL/GCE in 0.01 M PBS (pH 7.4) were investigated (Fig. 2B). In the case of ChOx/GCE no peaks were observed which is consistent with previous results (Li et al., 2011). However, a set of well-defined redox peaks were observed with the formal poetical −0.470 V versus Ag/AgCl at a scan rate of 100 mV/s when ChOx/GR/GCE was used (Fig. 2B, curve b). This corresponds to the electron transfer reactions of the FAD/$FADH_2$ couple of the electroactive center of ChOx (Cai and Chen, 2004). The electrochemical response of ChOx immobilized on GR–IL/GCE showed an improvement in peak currents without any significant shift in peak potentials (Fig. 2B, curve c). The peak currents of ChOx/GR/IL/GCE in 0.1 M PBS were investigated at different scan rates and the results are presented in Fig. S2. The direct proportionality between peak current and scan rate for both anodic and cathodic peaks (Fig. S2(B)) indicates a surface-confined process similar to the case of CAT. The peak potential separation of the ChOx was about 82 mV at a scan rate of 100 mV/s but this value increased with increasing the scan rate, suggesting that this redox reaction is quasi-reversible. The transfer coefficient (α) and heterogeneous electron transfer rate constant (k_s) for ChOx were determined using Laviron's equation and found to be 0.31 and 1.10 s^{-1}. This value for k_s is greater than the apparent heterogeneous electron transfer rate constant of ChOx at functionalized GR/graphite electrode 0.78 s^{-1} (Manjunatha et al., 2012), MWCNTs/GCE 0.027 s^{-1} (Yang et al., 2011b), hydrophobic ionic liquid (IL)/prussian blue/GCE 0.587 s^{-1} (Liu et al., 2013) and smaller than that obtained at potassium doped MWNT/GCE 2.28 s^{-1} (Li et al., 2011).

Previous reports (Salimi et al., 2005; Li et al., 2011) revealed that the electrochemical behavior of CAT and ChOx are pH dependent. Thus the effect of pH on the response of both electrodes (ChOx/GR/IL-GCE and CAT/GR–IL/GCE) was studied and their cyclic voltammograms are shown in Fig. S3. For both cases the reduction and oxidation peak potentials shift negatively with changing the pH from 2.4 to 8.4. The formal potentials of CAT and ChOx depend linearly on the pH value of the solution with the slops −62.1 mV/pH (R^2=0.996) and −63.7 mV/pH (R^2=0.996), respectively. This indicates that both the enzymes are involved in redox processes with equal number of electrons and protons. However, in the case of CAT a one-electron/one-proton process (Salimi et al., 2007) while for the electrochemical reaction of ChOx a two-electron/two-proton process (Li et al., 2011) have been reported according to the following equations:

$$CAT - Fe(III) + H^+ + e^- \leftrightarrow CAT - Fe(II)$$

$$ChOx(FAD) + 2H^+ + 2e^- \leftrightarrow ChOx(FADH_2)$$

From a practical point of view, pH 7.4 was selected for further studies because it is the physiological pH and enzymes are stable at this pH value.

The cyclic voltammetry was also used to study the electrochemical behavior of H_2O_2 on the modified electrodes. Fig. S4 shows the cyclic voltammograms of 0.01 M PBS (pH 7.4) in the absence (a) and presence (b) of 100 μM H_2O_2 at the GR–IL/GCE and scan rate of 100 mV/s. As shown in this figure, at the GR–IL/GCE no clear response for H_2O_2 was observed in the tested potential window (from 0.0 to −0.80 V). However, at the CAT/GR–IL/GCE, an obvious catalytic reduction peak was appeared at the potential of −0.50 V. The large increase in cathodic peak current and disappearance of anodic peak current with the addition of H_2O_2 indicates that the CAT/GR–IL/GCE has a good electrocatalytic activity towards H_2O_2 reduction. The similar experiment was carried out and the results showed that H_2O_2 was not electroactive at the ChOx/GR–IL/GC electrode. Therefore, the GR–IL/GC electrode modified with both ChOx and CAT can be used for sensitive

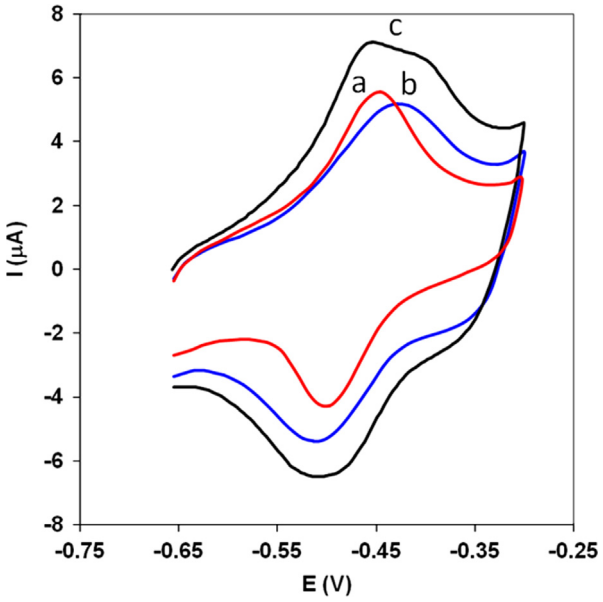

Fig. 3. Cyclic voltammograms of (a) CAT/GR-IL/GCE, (b) ChOx/GR-IL/GCE and ChOx/CAT/GR-IL/GCE in 0.01 M PBS (pH 7.4) at a scan rate of 100 mV/s.

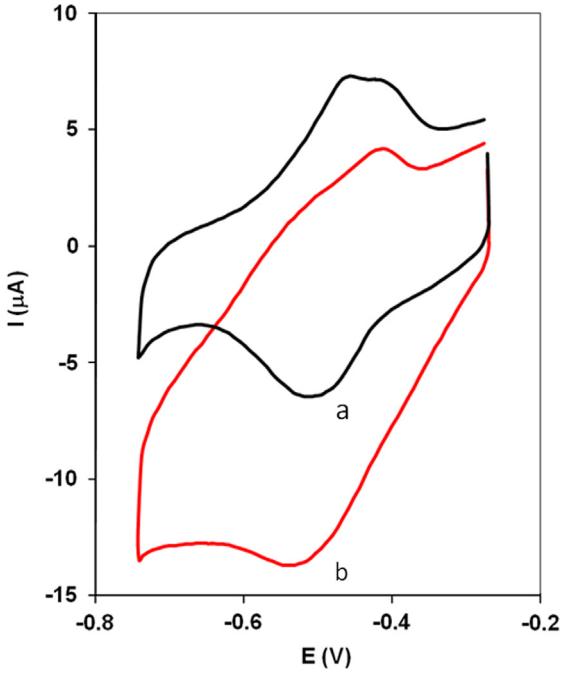

Fig. 4. Cyclic voltammograms of ChOx/CAT/GR–IL/GCE in 0.01 M PBS (pH 7.4) containing 0.2% (v/v) Triton X-100 and 0.5% (v/v) isopropanol in the absence (a) and in the presence (b) of 100 μM cholesterol.

detection of cholesterol. The catalytic oxidation of cholesterol by ChOx produces hydrogen peroxide which can be detected by immobilized CAT.

Fig. 3 compares the CVs recorded for the ChOx/GR–IL/GCE (a) CAT/GR–IL/GCE (b) and ChOx/CAT/GR–IL/GCE (c) in 0.01 M PBS (pH 7.4). As can be seen, the anodic and cathodic peaks of both CAT and ChOx are appeared at the same potential region, and therefore the cyclic voltammogram of ChOx/CAT/GR–IL/GCE is sum of the electrochemical signals of CAT and ChOx. These results clearly indicate that CAT has been successfully co-immobilized with ChOx on ChOx/CAT/GR–IL/GCE, and hence can be used as a cholesterol biosensor. Fig. 4 shows the CVs recorded for the ChOx/CAT/GR-IL/GCE in the absence (a) and presence (b) of 100 μM cholesterol in 0.01 M PBS (pH 7.4). Increasing the cathodic peak current of ChOx/CAT/GR–IL/GCE along with a decrease in the anodic peak current reveals the presence of an electrocatalytic process at the surface of the ChOx/CAT/GR–IL/GCE. The H_2O_2 which is produced from the catalytic oxidation of cholesterol by ChOx can be reduced by CAT in an electrocatalytic reaction. Hence, the electrochemical biosensor processes can be abbreviated as follows:

$$\text{Cholesterol} + O_2 \overset{\text{ChOx}}{\rightarrow} \text{Cholest} - 4 - \text{en} - 3 - \text{one} + H_2O_2$$

$$\text{CAT} - \text{Fe(III)} + H^+ + e^- \rightleftharpoons \text{CAT} - \text{Fe(II)} \quad \text{at the electrode}$$

$$H_2O_2 + \text{CAT} - \text{Fe(II)} \rightleftharpoons \text{CAT} - \text{Fe(III)} + H^+ + H_2O$$

The same mechanisms for the enzymatic reaction of cholesterol in the presence of cholesterol oxidase and electrocatalytic reduction of H_2O_2 in the presence of catalase have been reported previously (Wang et al., 2004; Xu and Wang, 2012).

3.3. Amperometric sensor response

In order to increase the sensitivity of the proposed method the amperometry under stirred conditions was selected instead of cyclic voltammetry; hence the amperometric experiments have been performed at a constant potential of −0.5 V and under continuous stirring. The amperometric responses and calibration curves for the biosensor under the optimized experimental conditions are shown in Fig. 5. The biosensor exhibited two linear ranges for cholesterol determination ranging from 0.25–5.0 μM and 5.0–215.0 μM with excellent correlation coefficients (> 0.99). The biosensor exhibited a rapid response to the changes in cholesterol concentration, and the stable current was obtained after 6 s. The detection limit was estimated to be about 0.05 μM for a signal-to-noise of 3.

The apparent Michaelis–Menten constant (K_M^{app}) for cholesterol was calculated using a Lineweaver–Burk plot according to the following equation:

$$\frac{1}{I} = \frac{1}{I_{max}} + \frac{K_M^{app}}{I_{max}[s]}$$

where I is the steady-state current, I_{max} is the maximum current obtained at saturated level of cholesterol, and [S] is the concentration of cholesterol. The I_{max} and K_M^{app} values were obtained from the graphical analysis of the Lineweaver–Burk plot ($1/I$ versus $1/[s]$). The values of I_{max} and were found to be 0.36 mA and 2.32 mM, respectively. The smaller K_M^{app} value means that the immobilized ChOx possesses higher affinity to cholesterol. Also, the value of K_M^{app} was calculated when ChOx was present in solution and it was found to be 0.40 mM that is much smaller than that obtained by the proposed electrode. Generally, the K_M^{app} of an immobilized enzyme will be larger than that of the free enzyme in solution due to the effect of the diffusion of substrate to the active sites (Chaplin and Bucke, 1990). On the other hand, the changes in the kinetic constants, K_M^{app} and I_{max} after immobilization of ChOx may be due to internal structural changes and restricted access to the active site (Chaplin and Bucke, 1990). However, the value obtained with the ChOx/CAT/GR–IL/GCE biosensor for cholesterol is smaller than or comparable with the previously reported values for the immobilization of ChOx on different substrates. Table 1 compares the characteristics of some reported cholesterol biosensors with the ChOx/CAT/GR–IL/GCE biosensor presented in this work.

3.4. Influence of interferences

One of the major problems in the detection of cholesterol using a biosensor is the interference from other biological species.

Therefore, the effect of some common interfering substances in cholesterol determination such as ascorbic acid, glucose, uric acid, acetaminophen, oxalic acid, citric acid and L-cysteine was investigated.

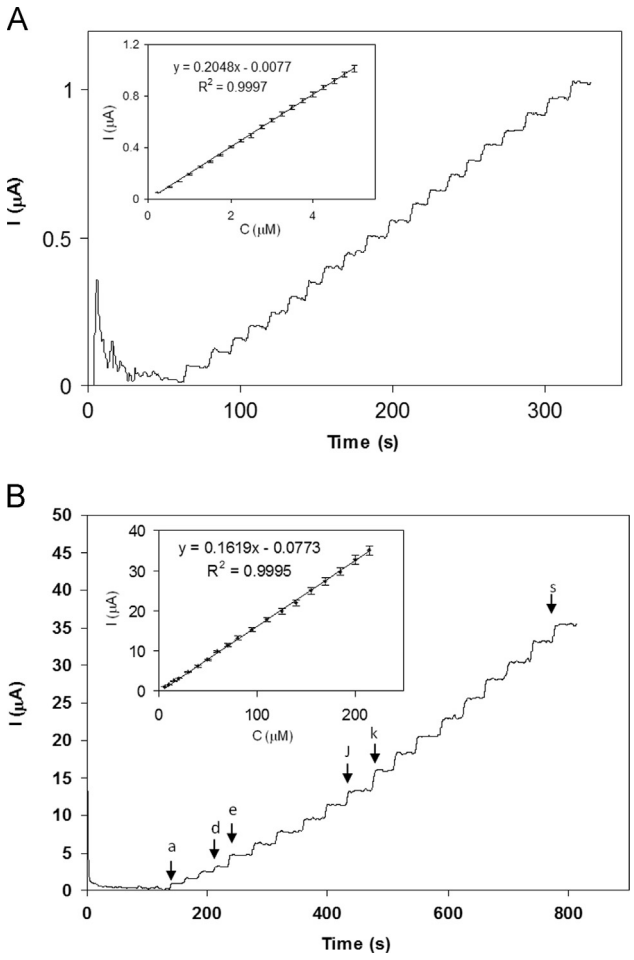

Fig. 5. The chronoamperometric response of the ChOx/CAT/GR–IL/GCE after successive additions of (A) 0.25 μM cholesterol and (B) (a–d) 5 μM, (e–j) 10 μM and (k–s) 15 μM cholesterol. Condition: 0.01 M PBS (pH 7.4) containing 0.2% (v/v) Triton X-100 and 0.5% (v/v) isopropanol at an applied potential of −0.5 V (versus Ag/AgCl).

At the applied potential of −0.5 V in a continuously stirred 0.01 M PB solution (pH 7.4), the addition of interfering substances up to 5 times greater than cholesterol concentration (20 μM) did not cause any significant change in the current response (Table S1). Thus, highly selective response to cholesterol was obtained under the experimental conditions presented here.

3.5. Repeatability, reproducibility, stability and application of the biosensor

At first, the repeatability of the biosensor towards 100 μM cholesterol solution at the ChOx/CAT/GR–IL/GCE was examined and the relative standard deviation, RSD was found to be 1.53% for eight successive assays. The reproducibility of five different fabricated electrodes was investigated in 0.01 M PBS solution (pH 7.4) containing 100 μM cholesterol. The relative standard deviation for cholesterol detection was found to be less than 5.6%. Long-term stability of the biosensor was also evaluated by measuring its performance after every few days. The biosensor shows high stability for cholesterol detection, and retains about 60% of its original response to cholesterol after 50 days of storage. This shows that GR–IL hybrid has good biocompatibility and maintains the biological activity of the immobilized enzyme. The decrease in current may be attributed to the deactivation or desorption of the immobilized enzyme from the electrode surface.

The proposed bienzymatic cholesterol sensor was used for the measurement of free cholesterol in human serum samples as a fundamental application. The serum samples were diluted in such a way that, cholesterol concentrations should fall in the working range of above mentioned electrode. The obtained data by the proposed sensor were compared with those obtained by a spectrophotometric method (Allain et al., 1974) and the results are summarized in Table S2. The results obtained were satisfactory with the recoveries ranging from 99.5% to 101.1%. Thus, we might utilize the proposed electrode as an efficient electrochemical biosensor for the preliminary determination of cholesterol in clinical diagnostics.

4. Conclusion

The results presented here demonstrate the possibility for the co-immobilization of ChOx and CAT on GR–IL modified glassy carbon electrode to conveniently construct a new bienzymatic

Table 1
Characteristics of the present ChOx/CAT/GR–IL/GCE cholesterol biosensor in comparison with the literature.

Electrode material	Linear range (μM)	Response. time (s)	LOD (μM)	Sensitivity (mA mM^{-1} cm^{-2})	I_{max} (mA)	K_M^{app} (mM)	Refs.
MWCNT–chitosan–Pt–cholesterol	$5.0–3.0 \times 10^2$	8	4.8	0.044	–	–	Tsai et al. (2008)
AuPt–Ch–IL/GCE	$50.0–11.2 \times 10^3$	7	10.0	0.090	–	0.24	Safavi and Farjami (2011)
Epoxy resin/Pt	1.0×10^3–8.0×10^3	25	1.0×10^3	–	0.009	5.00	Pundir et al. (2012)
PEO-co-PPy/ChOx/Pt foil	–	2–3	–	0.013	0.019	1.47	Yildiz et al. (2013)
ZnO/ChOx	$1.0–5.0 \times 10^3$	5	3.7×10^{-1}	0.024		4.70	Umar et al. (2009)
PEDOT/ChOx	–	150	400.0	0.010	0.004	3.40	Türkarslan et al. (2009)
MWCNT/ChOx	48.6–279.0		46.8	1.262	–	–	Yang et al. (2011a, b)
Poly(2-hydroxyethyl methacrylate)–polypyrrole	5.0×10^2–15.0×10^3	30	120.0	0.019	–	–	Brahim et al. (2001)
Polypyrrole film	1.0×10^3–8.0×10^3	–	–	0.015	–	9.80	Singh et al. (2004)
GR/nano-Pt/GCE	0.2–35.0	4	–	2.07	0.23	5.00	Dey and Raj (2010)
HRP/ChOx/pyrolytic graphite	40.0–270.0	30	–	–	–	6.00	Bongiovanni et al. (2001)
Pt–ZnO	0.5–15.0	5	–	1.886	–	–	Ahmad et al. (2010)
ChOx/CAT/GR–IL/GCE	2.5×10^{-1}–215.0	6	5.0×10^{-2}	4.163	0.360	2.32	This work

cholesterol biosensor. The enzymes were well immobilized on the electrode surface and retained satisfactory enzymatic catalytic activities. Direct electron communication between CAT and electrode is easily bridged by the GR–IL so that the selective determination of cholesterol with minimal interference was realized. The cholesterol biosensor also presented fast response, preferable linear range accompanied with favorable sensitivity and detection limit. The utility of such a biosensor for detection of free cholesterol shows great promise for the use in invitro measurements.

Appendix A. Supporting information

Supplementary data associated with this article can be found in the online version at http://dx.doi.org/10.1016/j.bios.2013.09.074.

References

Ahmad, M., Pan, C., Gan, L., Nawaz, Z., Zhu, J., 2010. J. Phys. Chem. C 114, 243–250.
Ahmadalinezhad, A., Chen, A., 2011. Biosens. Bioelectron. 26, 4508–4513.
Ahn, K.W., Sampson, N.S., 2004. Biochemistry 43, 827–836.
Allain, C.C., Poon, L.S., Chan, C.S.G., Richmond, W., Fu, P.C., 1974. Clin. Chem. 20, 470–475.
Bard, A.J., Faulkner, L.R., 2001. Electrochemical Methods. John Wiley and Sons, New York.
Bongiovanni, C., Ferri, T., Poscia, A., Varalli, M., Santucci, R., Desideri, A., 2001. Bioelectrochemistry 54, 17–22.
Brahim, S., Narinesingh, D., Guiseppi-Elie, A., 2001. Anal. Chim. Acta 448, 27–36.
Cai, C., Chen, J., 2004. Anal. Biochem. 332, 75–83.
Chaplin, M.F., Bucke, C., 1990. Enzyme Technology. Cambridge University Press, UK.
Chen, L., Lu, G., 2006. J. Electroanal. Chem. 597, 51–59.
Chen, X.H., Xie, H., Kong, J.L., Deng, J.Q., 2001. Biosens. Bioelectron. 16, 115–120.
Choi, B.G., Park, H.S., 2012. ChemSusChem 5, 709–715.
Dey, R.S., Raj, C.R., 2010. J. Phys. Chem. C 114, 21427–21433.
Ferapontova, E.E., Grigorenko, V.G., Egorov, A.M., Borchers, T., Ruzgas, T., Gorton, L., 2001. Biosens. Bioelectron. 16, 147–157.
Gopalana, A.I., Leea, K.P., Ragupathya, D., 2009. Biosens. Bioelectron. 24, 2211–2217.
Gu, H.Y., Yu, A.M., Chen, H.Y., 2001. J. Electroanal. Chem. 516, 119–126.
Hall, S.B., Khudaish, E.A., Hart, A.L., 2000. Electrochim. Acta 45, 3573–3579.
Hapiot, P., Lagrost, C., 2008. Chem. Rev. 108, 2238–2264.
Hojo, K., Hakamata, H., Kusu, F., 2011. J. Chromatogr. B 879, 751–755.
Iannlello, R.M., Yacynych, A.M., 1981. Anal. Chem. 53, 2090–2095.
Kang, X.H., Wang, J., Wu, H., Aksayc, I.A., Liu, J., Lin, Y.H., 2009. Biosens. Bioelectron. 25, 901–905.
Krug, A., Gobel, R., Kellner, R., 1994. Anal. Chim. Acta 287, 59–64.
Laviron, E., 1979. J. Electroanal. Chem. 101, 19–28.
Li, J., Guo, S.J., Zhai, Y.M., Wang, E.K., 2009. Electrochem. Commun. 11, 1085–1088.
Li, Y.M., Chen, X.T., Li, J., Liu, H.H., 2004. Electrochim. Acta 49, 3195–3200.
Li, X.-R., Xu, J.-J., Chen, H.-Y., 2011. Electrochim. Acta 56, 9378–9385.
Liu, S., Dai, Z., Chen, H., Ju, H., 2004. Biosens. Bioelectron. 19, 963–969.
Liu, S.Q., Ju, H.X., 2002. Anal. Biochem. 307, 110–116.
Liu, X., Nan, Z., Qiu, Y., Zheng, L., Lu, X., 2013. Electrochim. Acta 90, 203–209.
Manjunatha, R., Suresh, G.S., Melo, J.S., D'Souza, S.F., Venkatesha, T.V., 2012. Talanta 99, 302–309.
Marcano, D.C., Kosynkin, D.V., Berlin, J.M., Sinitskii, A., Sun, Z., Slesarev, A., Alemany, L.B., Lu, W., Tour, J.M., 2010. ACS Nano 4, 4806–4814.
Melik-Adamyan, W.R., Barynin, V.V., Vagin, A.A., Borisov, V.V., Vainshtein, B.K., Fita, I., Murthy, M.R.N, Rossmann, M.G., 1986. J. Mol. Biol. 188, 63–72.
Nakaminami, T., Kuwabata, S., Yoneyama, H., 1997. Anal. Chem. 69, 2367–2372.
Novoselov, K.S., Geim, A.K., Morozov, S.V., Jiang, D., Zhang, Y., Dubonos, S.V., Grigorieva, I.V., Firsov, A.A., 2004. Science 306, 666–669.
Pumera, M., Smíd, B., Veltruská, K., 2009. J. Nanosci. Nanotechnol. 9, 2671–2676.
Pundir, C.S., Narang, J., Chauhan, N., Sharma, P., Sharma, R., 2012. Indian J. Med. Res. 136, 633–640.
Safavi, A., Farjami, F., 2011. Biosens. Bioelectron. 26, 2547–2552.
Safavi, A., Maleki, N., Farjami, E., Mahyari, F.A., 2009. Anal. Chem. 81, 7538–7543.
Salimi, A., Noorbakhsh, A., Ghadermarz, M., 2005. Anal. Biochem. 344, 16–24.
Salimi, A., Sharifi, E., Noorbakhsh, A., Soltanian, S., 2007. Biophys. Chem. 125, 540–548.
Shan, C.S., Yang, H.F., Han, D.X., Zhang, Q.X., Ivaska, A., Niu, L., 2010. Biosens. Bioelectron. 25, 1504–1508.
Shan, C.S., Yang, H.F., Song, J.F., Han, D.X., Ivaska, A., Niu, L., 2009. Anal. Chem. 81, 2378–2382.
Singh, S., Chaubey, A., Malhotra, B.D., 2004. Anal. Chim. Acta 502, 229–234.
Sugano, M., Beynen, A.C., 1990. Dietary Proteins, Cholesterol Metabolism and Atherosclerosis. Karger, New York.
Tan, L., Zhou, K.G., Zhang, Y.H., Wang, H.X., Wang, X.D., Guo, Y.F., Zhang, H.L., 2010. Electrochem. Commun. 12, 557–560.
Tsai, Y., Chen, S., Lee, C., 2008. Sens. Actuators B 135, 96–101.
Tunckol, M., Durand, J., Serp, P., 2012. Carbon 50, 4303–4334.
Türkarslan, Ö., Kayahan, S.K., Toppare, L., 2009. Sens. Actuators B 136, 484–488.
Umar, A., Rahman, M.M., Vaseem, M., Hahn, Y.B., 2009. Electrochem. Commun. 11, 118–121.
Wang, L., Wang, J., Zhou, F., 2004. Electroanalysis 16, 627–632.
Wong, W.W., Hachey, D.L., Clarke, L.L., Zhang, S., Liaurador, M., Piond, W.G., 1994. Appl. Radiat. Isot. 45, 529–533.
Wu, Y., Shen, Q., Hu, S., 2006. Anal. Chim. Acta 558, 179–186.
Xiao, F., Zhao, F.Q., Mei, D.P., Mo, Z.R., Zeng, B.Z., 2009. Biosens. Bioelectron. 24, 3481–3486.
Xu, Y., Wang, E., 2012. Electrochim. Acta 84, 62–73.
Yang, M.H., Choi, B.G., Park, H.S., Park, T.J., Hong, W.H., Lee, S.Y., 2011a. Electroanalysis 23, 850–857.
Yang, H.F., Shan, C.S., Li, F.H., Han, D.X., Zhang, Q.X., Niu, L., 2009. Chem. Commun. 26, 3880–3882.
Yang, J.-Y., Li, Y., Chen, S.-M., Lin, K.-C., 2011b. Int. J. Electrochem. Sci. 6, 2223–2234.
Yao, T., Satomura, M., Nakahara, T., 1995. Electroanalysis 7, 143–146.
Yildiz, H.B., Demirkol, D.O., Sayin, S., Yilmaz, M., Koysuren, O., Kamaci, M., 2013. J. Macromol. Sci., Part A: Pure Appl. Chem. 50, 1075–1084.
Zhang, B., Zhang, Z., Wang, B., Yan, J., Li, J., Cai, S.M., 2001. Acta Chim. Sin. 59, 1932–1936.
Zhao, C., Wan, L., Jiang, L., Wang, Q., Jiao, K., 2008. Anal. Biochem. 383, 25–30.
Zhou, H., Lu, T.H., Shi, H.X., Dai, Z.H., Huang, X.H., 2008. J. Electroanal. Chem. 612, 173–178.
Zhou, M., Zhai, Y.M., Dong, S.J., 2009. Anal. Chem. 81, 5603–5613.
Zhu, H., Lu, X., Li, M., Shao, Y., Zhu, Z., 2009. Talanta 79, 1446–1453.